

**Termination control of electronic phases in oxide thin films
and interfaces: LaAlO₃/SrTiO₃(001)**

R. Pentcheva¹, R. Arras¹, K. Otte¹, V. G. Ruiz López¹, and W. E. Pickett²

¹ DEPARTMENT OF EARTH AND ENVIRONMENTAL SCIENCES, SECTION CRYSTALLOGRAPHY AND CENTER OF NANOSCIENCE, UNIVERSITY OF MUNICH, THERESIENSTR. 41, 80333 MUNICH, GERMANY

²DEPARTMENT OF PHYSICS, UNIVERSITY OF CALIFORNIA, DAVIS, ONE SHIELDS AVENUE, DAVIS, CA 95616, U.S.A.

ABSTRACT. oxide interfaces; DFT; magnetic thin oxide films; metal-insulator transition; metal-insulator contacts; Schottky barrier

A wealth of intriguing properties emerge in the seemingly simple system composed of the band insulators LaAlO_3 and SrTiO_3 such as a quasi two dimensional electron gas, superconductivity and magnetism. In this paper we review the current insight obtained from first principles calculations on the mechanisms governing the behavior of thin LaAlO_3 films on $\text{SrTiO}_3(001)$. In particular, we explore the strong dependence of the electronic properties on the surface and interface termination, the finite film thickness, lattice polarization and defects. A further aspect that is addressed is how the electronic behavior and functionality can be tuned by a SrTiO_3 capping layer, adsorbates and metallic contacts. Lastly, we discuss recent reports on the coexistence of magnetism and superconductivity in this system for what they might imply about the electronic structure of this system.

1. Introduction

The advance of thin film growth techniques like pulsed laser deposition (PLD) and molecular beam epitaxy (MBE) allows the fabrication of single terminated oxide interfaces on the atomic scale. Understanding the novel phenomena arising in these artificial materials is not only of fundamental interest, but is also relevant for the development of future electronics and spintronics devices. One system that has attracted most of the interest so far is comprised of the simple band insulators LaAlO_3 (LAO) and SrTiO_3 (STO) where a quasi two-dimensional electron gas (q2DEG) [1], superconductivity [2], magnetism [3] and even signatures of their coexistence [4, 5, 6] have been reported. A further feature of interest and potential importance is that the electronic properties can be tuned by the LAO thickness and the system undergoes a transition from insulating to conducting behavior around four monolayers (ML) LAO [7]. This insulator-metal transition (MIT) can be controlled reversibly via an electric field, e.g. by an atomic force microscopy (AFM) tip [8, 9, 10] and several electronic devices based on this feature have been proposed [11, 12]. The electronic properties can be further tuned by an additional STO capping layer that triggers the MIT already at 2ML thereby stabilizing an electron-hole bilayer [13]. The electronic properties show a strong dependence on the growth conditions, with a variation in sheet resistance by seven orders of magnitude with the oxygen partial pressure in the PLD chamber.[3] This enormous change implies that oxygen defects play a controlling role during low pressure growth.

Extensive theoretical and experimental efforts aim at explaining the origin of these interfacial phenomena. A central feature is the polar discontinuity that emerges at the interface: in the (001) direction LAO consists of charged $(\text{LaO})^+$ and $(\text{AlO}_2)^-$ planes, while in STO formally neutral $(\text{SrO})^0$ and $(\text{TiO}_2)^0$ planes alternate. Because both cations change across the interface, two distinct interfaces can be realized: an electron doped *n*-type with a LaO layer next to a TiO_2 layer and a hole-doped *p*-type interface with a SrO and AlO_2 next to each other. Assuming formal ionic charges, the electrostatic potential produced by an infinite stack of charged planes would grow without bound, a phenomenon known as the *polar catastrophe* [14, 15]. This polar catastrophe cannot of course actually occur, and it may be avoided in several ways: A mechanism also common to semiconductors is an *atomic reconstruction* via introduction of defects or adsorbates. In transition metal oxides electronic degrees of freedom may lead to an alternative compensation mechanism, i.e. an *electronic reconstruction*. The latter can give rise to exotic electronic states, for example

the observed 2D conductivity in LAO/STO, charge/spin/orbital order, excitonic or superconducting phases. A further question that arises is whether a thin film of LAO with only a few layers approaches the regime of the *polar catastrophe*. Sorting out the many possibilities is challenging due to the strong dependence on growth method and conditions.

In this paper we review the progress made so far in understanding the mechanisms that determine the electronic behavior of LAO/STO(001) based on density functional theory calculations. For more detailed reviews on the experimental and theoretical work the reader is referred to [16, 17, 18, 19, 20]. In particular we address finite size effects and the role of electrostatic boundary conditions [21] in thin LAO films on STO(001). We first discuss intrinsic mechanisms that arise at defect-free *n*- and *p*-type interfaces providing a possible explanation for the thickness dependent insulator-to-metal transition (IMT). Moreover, we explore the effect of the surface termination on the band diagram. In Sections 3 and 5 we address the role of a STO capping layer and a metallic electrode. A controversially discussed issue is the presence of an internal potential buildup within the LAO film, as predicted by DFT calculations on LAO/STO(001) with abrupt interfaces. While recent AFM experiments provide evidence for such an internal field in terms of a polarity-dependent asymmetry of the signal [22], x-ray photoemission studies [23, 24, 25] have not been able to detect shifts or broadening of core-level spectra that would reflect an internal electric field. This discrepancy implies that besides the electronic reconstruction, extrinsic effects play a role, e.g. oxygen defects [26, 27], adsorbates such as water or hydrogen [28] or cation disorder [29, 30]. An overview of the current theoretical understanding of the role of such extrinsic mechanisms is provided in Section 4. Finally, in Section 6 we address recent reports on the coexistence of superconductivity and ferromagnetism in LAO/STO - a phenomenon which may be very helpful in understanding the underlying electronic structure in these nanoscale systems.

2. Polar oxide films on a nonpolar substrate: LAO/STO(001)

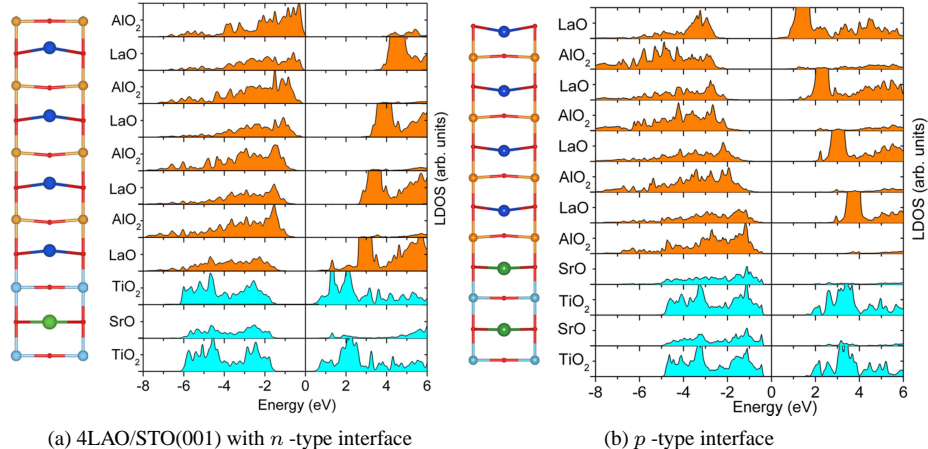


FIGURE 1. (Color online) Side view of the relaxed structure and layer resolved DOS of 4LAO/STO(001) with a (a) *n*-type and (b) *p*-type interface.

An intriguing experimental finding in LAO/STO(001) is the thickness dependent insulator-to-metal transition in thin LAO films on STO(001) [7]. Density functional theory calculations (DFT) demonstrate that an internal electric field emerges in thin polar LAO overayers on STO(001) [31, 32, 33, 18]. As shown in the layer resolved density of states (DOS) of a 4ML LAO film on STO(001) with an *n*-type interface (Fig. 1a), this is expressed in an upward shift of the O₂*p* bands as they get closer to the surface. Interestingly, a large electric field of opposite sign arises in an analogous manner in a defect free 4ML LAO/STO(001) overlayer with a *p*-type interface (Fig. 1b). The internal electric field of the polar LAO film is screened to a large degree (but not exactly) by a strong lattice polarization. As can be seen from the side view of the relaxed structure in Fig. 1a and the anion-cation buckling displayed in Fig. 2, for an *n*-type interface this lattice polarization is characterized by a strong outward shift of La by 0.2-0.3 Å and buckling in the subsurface AlO₂ layers while the surface layer shows similar relaxations for anions and cations. Experimental evidence for such a lattice polarization within the LAO film seems contradictory. Segal *et al.* [23] and Chambers *et al.* [25] saw no evidence for the expected core level shifts due to an internal field. However, evidence has been recently obtained for the internal field by surface x-ray diffraction (SXRD) determination of the lattice polarization, by Pauli *et al.* [34]. This latter study detected also a dependence of the lattice response on the LAO thickness with a maximum buckling in a 2 ML LAO film. This indicates possibly a stronger role of cation interdiffusion or higher affinity for adsorbates in the thicker films. Such extrinsic mechanisms can reduce the internal potential and thereby the lattice polarization (see discussion in Section 4).

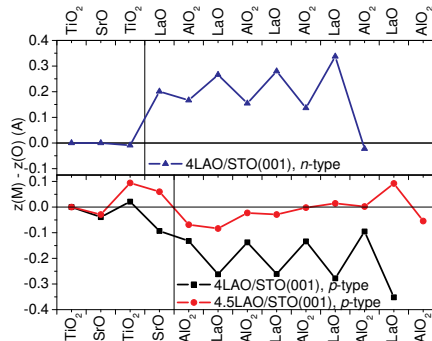


FIGURE 2. (Color online) Oxygen-cation buckling in 4LAO/STO(001) with an *n*- (blue triangles) and a *p*-type interface (black squares), as well as 4.5LAO/STO(001) with a *p*-type interface (red circles).

The lattice relaxation has a crucial effect on the electronic properties: if the atoms are fixed at their ideal bulk positions, all systems are metallic. The lattice polarization in the relaxed system allows several layers of LAO to remain insulating with a band gap of 1.7 eV for 1ML LAO/STO(001) and a gradual decrease by ~ 0.4 eV per added LAO ML. Finally, at around 5 monolayers of LAO an electronic reconstruction takes place. However, the closing of the band gap is “indirect” in real space as it is due to overlap of the valence band defined by the O₂*p* band in the surface layer and the conduction band marked by Ti 3*d* states at the interface. Consequently, the carrier density is much lower than the one expected if 0.5*e* were transferred to the interface. Furthermore, the results suggest carriers of two different types: electrons at the interface and holes in the surface layer. We

will return to the possibility of excitonic effects later when discussing the role of a STO capping layer in Section 3.

For 4LAO/STO(001) with a *p*-type interface the ionic relaxations are of similar magnitude but of opposite sign (note the inward relaxation of the La-ions and the anion cation buckling shown in Fig. 2). A very similar thickness dependent insulator-to-metal transition is expected which involves however different states: La 5*d* states in the surface LaO layer and O2*p* states at the interface. In experiments, the *p*-type interface has been found so far insulating [1] and has therefore attracted much less attention. The analysis of O K-edge spectra by Nakagawa, Hwang, and Muller suggested that compensation takes place via oxygen vacancies, [35] that is, by atomic reconstruction. Still, the results above and by [31] show that provided defect-free LAO/STO IFs with a *p*-type interface can be realized they would exhibit just as interesting thickness dependent properties as the ones for the *n*-type IF. Therefore, the LAO/STO *p*-type interface deserves more study.

Dependence on the surface termination So far we have considered stoichiometric 4ML

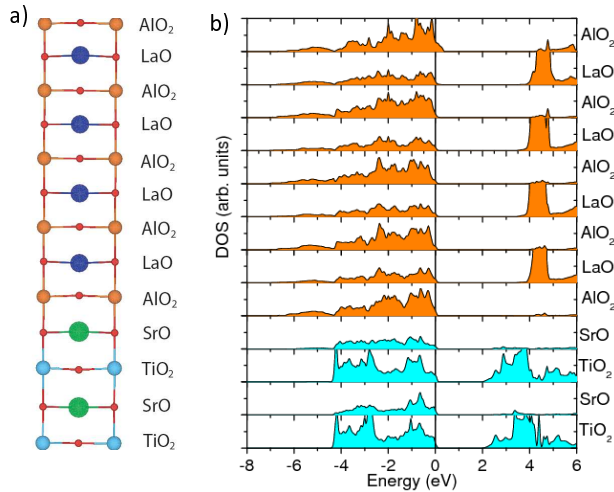


FIGURE 3. (Color online) a) side view of the relaxed structure and b) layer resolved DOS of 4.5LAO/STO(001) with a *p*-type interface and a AlO₂ termination.

LAO films on STO(001). What happens if we add a further LaO (*n*-type) or AlO₂ (*p*-type) layer on top of the surface? For the *p*-type interface this case is shown in Fig. 3. The system differs from Fig. 1b only by a single AlO₂ surface layer but the effect is substantial: the internal electric field is canceled (and consequently no lattice polarization is observed) and the surface layer is *p*-type conducting. Furthermore, the valence bands in the deeper layers are aligned in STO and LAO at the Fermi level, while there is an offset of the conduction bands due to the different sizes of the LAO and STO band gaps. [Note that a neutral AlO₂ layer was added: Al³⁺O₂[−] plus a hole.]

An analogous effect was studied by Pavlenko and Kopp [36] for LAO/STO(001) with an *n*-type interface and a LaO surface termination. Note that here both the surface and the interface are electron doped. Not surprisingly, the system is found to be metallic for 2.5 and 3.5 ML LAO with finite occupation of Ti 3*d*_{xy} states in the interface layer and La 5*d*_{x²-y² states in the surface layer. The authors interpreted the surface La5*d* occupation as a result of surface tensile stress. While the latter influences e.g. the vertical relaxation of}

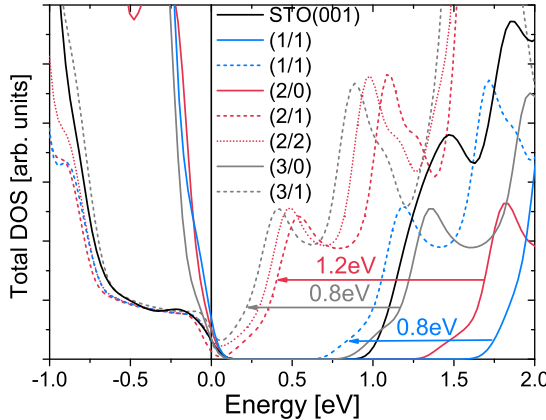


FIGURE 4. (Color online) Total density of states (LDOS) n LAO/STO(001), capped by m STO layers. Note that the band gap closes for $n > 2$ ML and the effect of the first STO layer is most pronounced.

ions, the polarity discontinuity at the surface and interface is likely to be the dominating effect.

3. Influence of a STO capping layer

In contrast to the sharp insulator-to-metal transition in LAO films on STO, Huijben et al. [37] observed a much smoother transition that starts already at 2ML LAO if the latter is covered by a nonpolar STO layer. The total DOS of n ML LAO/STO(001) covered by m layers of STO [denoted in the following as (n/m)] is displayed in Fig. 4. The DFT results reveal that for $n = 2$ ML already a single STO capping layer leads to an insulator-to-metal transition. Increasing the number of STO capping layers m or LAO layers n enhances the DOS at the Fermi level, but the first STO capping layer has the most dramatic effect, reducing the band gap by ~ 1.0 eV.

In order to gain more insight into the mechanism of closing of the gap, we analyze first the lattice relaxations. Fig. 5 shows the cation-anion displacements in m STO/ n LAO/STO(001). We observe slight reduction in the buckling within the LAO film compared to the (2/0) system and a polarization within the STO layer. The relaxation pattern in the STO capping layer is in fact similar to the one of the STO(001) surface [38] (for comparison the relaxations at a STO(001) surface are added to Fig. 5). However, the total contribution of the STO capping layer is small as the ionic dipole moments of the SrO and TiO₂ layers are of opposite sign (negative dipole moment in the surface TiO₂ layer and a positive one in the subsurface SrO layer) and nearly cancel. The results show that the ionic contribution to the dipole moment in m STO/ n LAO/STO(001) scales with the number n of LAO layers. Hence, the total ionic part of the dipole moment of m STO/ n LAO/STO(001) scales with the number n of LAO layers and increases roughly by 1 eÅ per added LAO layer.

The impact of the STO capping layer turns out to be of electronic origin: Fig. 6 shows the layer resolved DOS of (2/0)-dotted and (2/1)-line aligned at the bottom of the Ti3d interface band. Both in the capped and uncapped system the O2p bands within the LAO film exhibit a gradual upward shift of 0.4 eV per LAO as they approach the surface. In the capped system, there is an additional strong shift/broadening of the O 2p band in the

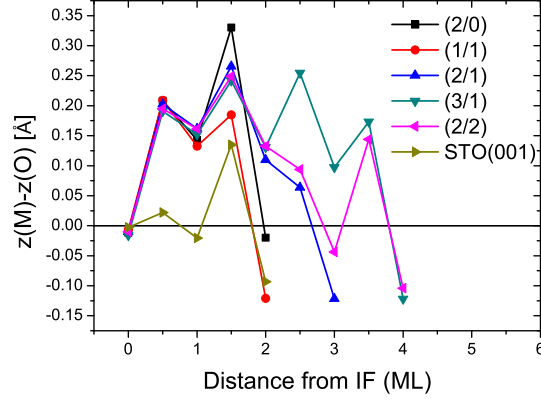


FIGURE 5. (Color online) Cation-anion vertical buckling in m STO/ n LAO/STO(001).

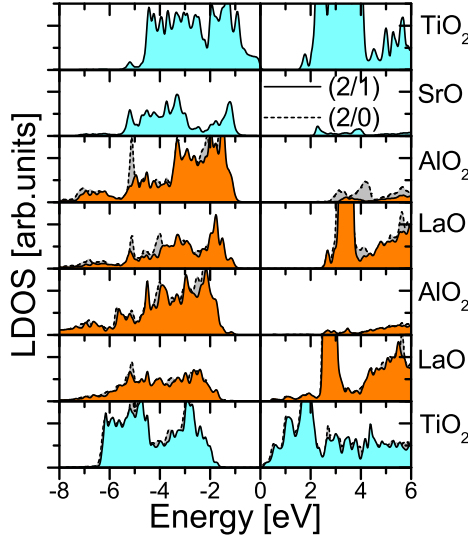


FIGURE 6. (Color online) Layer resolved density of states (LDOS) of 2LAO/STO(001) with and without a single STO capping layer, showing insulating behavior.[13]

surface TiO_2 layer of ~ 0.8 eV that gives rise to a closing of the band gap and an electronic reconstruction [13].

Indeed, the band structure in Fig. 7 shows a dispersive $\text{O}2p$ surface band, similar to a surface state in STO(001) [38, 39], that extends 0.8 eV above the subsurface $\text{O}2p$ band and marks the top of the valence band at the M point of the Brillouin zone. On the other hand the bottom of the conduction band lies at the Γ point and is determined by Ti 3d states in the interface layer. Thus the closing of the band gap is indirect both in real and reciprocal space. Increasing the number of LAO and STO capping layers enhances the overlap of the valence and conduction bands at the Fermi level.

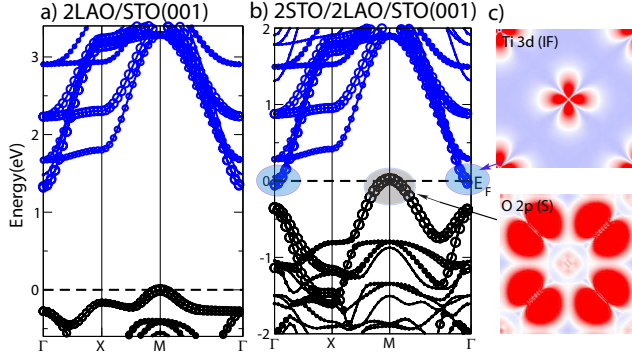


FIGURE 7. (Color online) Band structure of a) 2LAO/STO(001) and b) 2STO/2LAO/STO(001); c) integrated electron density around the bottom of the conduction band at Γ and the top of the valence band at M , showing Ti $3d_{xy}$ and O $2p\pi$ states, respectively in the two overlapping bands. Adapted from Ref.[13].

The electron density distribution integrated between -0.6 and 0.0 eV shows electrons of Ti $3d_{xy}$ character in the interface layer and holes in the O $2p\pi$ bands at the surface. From the curvature of the electron and hole bands at the Γ and M points we determine a significantly higher effective mass of the holes ($1.4 m_e/1.2 m_e$ in the uncapped/capped system, respectively) than for the lighter electrons ($0.4 m_e$). The presence of two types of carriers with different mobilities is confirmed in Hall and magnetoresistance measurements [13] where the data between 0-100 K can be fitted only by using a two-band model with one hole and one electron band. Photoemission experiments give further evidence for the presence of holes in the surface layer [13]. Thus the presence of a nonpolar oxide capping layer seems to stabilize the system w.r.t. surface defects and adsorbates that are likely to eliminate holes in the uncapped systems.

In contrast, when the system is terminated by a SrO layer (using a 1.5 ML STO overlayer) the layer resolved DOS in Fig. 8 shows that the band gap of ~ 1 eV of the uncapped (2/0) system is preserved. The reduction of the band gap is solely due to the potential build up within the LAO film, while the valence band (VB) of the STO capping layer aligns with the VB in the top AlO_2 layer without the surface state characteristic of the TiO_2 -terminated capping layer. This system exhibits a behavior that is closer to what one would expect when adding a “nonpolar” oxide overlayer on top of LAO/STO(001).

4. Role of lattice defects and adsorbates

Cationic intermixing The systems considered so far contained abrupt interfaces. However, several studies suggest significant cation intermixing at the interface [29, 30, 34]. Intermixing has been discussed as an alternative mechanism to the electronic reconstruction to compensate polarity, but the role of intermixing in canceling the potential divergence is questioned [40]. Qiao *et al.* [30] proposed as main sources of defects deviations from a 1:1 La:Sr ratio due to strong angular dependence during the PLD process, Sr vacancy formation, and La interdiffusion into the STO substrate. They investigated La \rightarrow Sr and Al \rightarrow Ti both near and far from the interface using up to 4 ML LAO on a 6 ML thick STO substrate in a $c(2 \times 2)$ lateral unit cell. The DFT results indicate that coupled La-Sr, Al-Ti exchange processes involving both the surface and interface region lower the energy of the system and the energy gain is dependent on the LAO thickness, being ~ 1.0 eV for $n = 3$ LAO

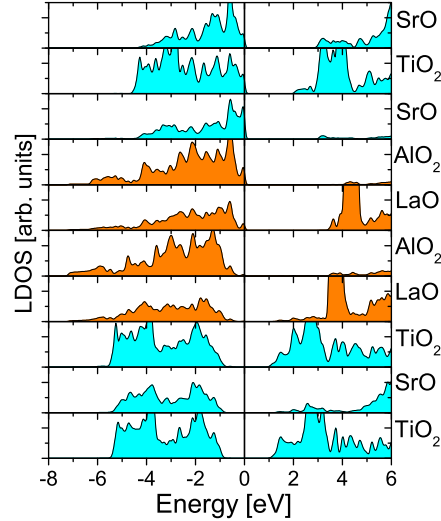


FIGURE 8. (Color online) Layer resolved density of states (LDOS) of a SrO terminated 1.5ML STO/2LAO/STO(001), showing insulating behavior.

and ~ 1.6 eV for $n = 4$ LAO layers, respectively. A comparison of the calculated and measured VBO was used as a further criterion to prove the presence of intermixing.

Pauli et al. [34] performed SXRD experiments and DFT calculations on films with thickness between 2-5 ML LAO. The experimental data indicated an 80% complete surface layer with 20% of a layer on top of that. Furthermore the results were consistent with cation intermixing exceeding 5% throughout 3 ML around the interface layer. In contrast to the study of Qiao et al. [30], DFT calculations on abrupt and intermixed interfaces did not show significant differences in electronic behavior.

Oxygen defects As mentioned in the introduction, a number of experimental studies have shown the strong influence of the oxygen partial pressure during deposition or post-deposition annealing on the transport properties. Despite its importance, there are only a few studies that have addressed the role of oxygen vacancies. Cen et al. [8] considered a 3ML LAO/STO(001) with a vacancy in the surface AlO_2 layer and found a dramatic difference of the electronic properties with reduction/cancellation of the electric field within the LAO film and an accumulation of carriers at the interface, in contrast to the insulating defect-free 3 ML LAO/STO(001). Chen, Kolpak and Beiji [41] modeled LAO/STO superlattices with the *p*-type interface and observed that oxygen vacancies are repelled from the interface towards bulk STO. On the other hand, Zhong, Xu and Kelly [26] studied oxygen vacancies in an $(\text{LAO})_m/(\text{STO})_m$ superlattice with alternating *n*- and *p*-type interfaces. In contrast to Chen et al. [41], they found that the formation energy of vacancies is lowest at the *p*-type interface and ~ 2 eV higher at the *n*-type interface with a nonlinear dependence in between. Furthermore, the vacancy formation tends to be more favorable in BO_2 -layers than in AO-layers of the perovskite lattice. The formation energy at the *p*-type interface becomes negative with respect to the one in STO bulk at a critical thickness $m = 3 - 4$ MLs. The electrons released by the vacancy are transferred to the conduction band minimum at the *n*-type interface (with a significant orbital polarization in the interface and more distant TiO_2 layers) while the *p*-type interface is insulating. This result implies separation between regions where impurity scattering takes place and regions of enhanced carrier density. The

authors also observed that the vacancy formation reduces the core-level shifts within the superlattice and proposed this as a possible explanation of the lacking broadening in XPS measurements [23, 24, 25].

Zhang et al. [42] studied the formation of vacancies in thin LAO overlayers on STO(001) using an asymmetric setup with dipole correction, and varied the position of the vacancies within the LAO film. Note that only the Γ -point was used for integration within the Brillouin zone. In systems with a *p*-type interface vacancies are formed preferentially at the interface, thereby compensating the valence discontinuity and leaving the system insulating. In contrast, for systems with an *n*-type interface the formation energy was significantly higher and tend to be formed rather in the surface LAO layer than at the interface. This has two consequences: it compensates the *p*-type surface AlO_2 -layer and enhances the carrier density at the interface. Based on a phenomenological electrostatic model, Bristowe, Littlewood and Artacho [27] showed that there is a critical thickness for surface vacancy formation, in agreement with DFT calculations [43]. Furthermore, they proposed that surface defects generate a trapping potential for carriers whose strength depends on the LAO-film thickness.

DFT calculations [44] introducing an oxygen vacancy in the interface TiO_2 layer within a 2×1 lateral unit cell indicate spin-polarization of the carriers in the Ti 3d band and propose this as a possible explanation of the recently reported coexistence of ferromagnetism and superconductivity in the LAO/STO(001) system (see also discussion in Section 6). Further studies are necessary to explore lower concentrations of vacancies and other thermodynamically more stable sites for the vacancy (e.g. in the surface AlO_2 -layer).

H-adsorption In most of the experiments so far, the samples are exposed to air, thus the interfacial properties can be significantly affected by adsorbates. These are considered as a possible origin of reversible writing and erasing of conducting regions on LAO/STO(001) by an AFM tip [8]. Son et al [33] investigated the H-adsorption using DFT-PBE. They found that the adsorption energy increases with LAO thickness and that beyond a critical thickness of ~ 5 ML the energy gain exceeds the energy needed for H_2 or H_2O dissociative adsorption. An interesting feature is the planar adsorption geometry with the H-O bond being nearly parallel to the surface reflecting a maximized overlap between the H 1s orbitals and the planar O 2p_π states. H is found to donate electrons to the STO conduction band. Furthermore, size and sign of the internal potential buildup can be tuned by the H concentration on the surface: e.g. the latter is exactly canceled for a (2×1) surface unit cell (this coverage corresponds to 0.5e transfer per (1×1) lateral unit cell). The impact of H-adsorption bears strong parallels to the influence of a metallic contact layer on the interfacial properties that will be discussed below. The influence of further adsorbates like water has not been considered so far but needs to be addressed in order to obtain a comprehensive picture of all effects that may determine the properties of LAO/STO(001).

5. Impact of metallic contacts on the electronic behavior of LAO/STO(001)

In Sections 3 and 4 we have seen that the presence of a nonpolar oxide overlayer or defects can significantly alter the electronic properties of the LAO/STO system. For device applications metallic overlayers are important and several experimental studies have used setups with metallic contacts on LAO/STO [10, 45, 46]. The coupling between metallic thin films and semiconductors or ferroelectric oxides have been widely studied [47, 48, 49, 50, 51]. In order to gain understanding in the impact of metallic contacts on the electronic behaviour of an oxide interface, we have recently performed DFT calculations on Al-, Ti-,

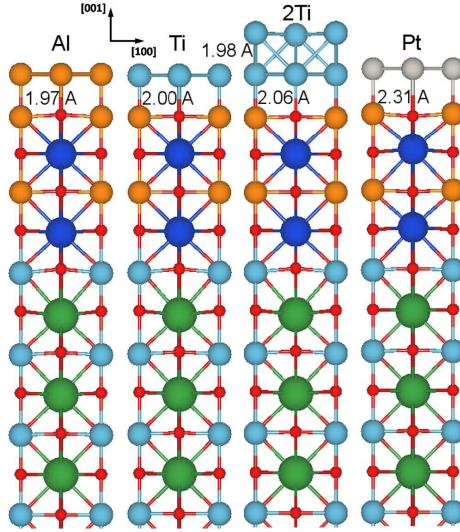


FIGURE 9. Side view of the relaxed structures for M/LAO/STO systems (M = Al, Ti, 2Ti and Pt). Only half of our symmetric slab is shown. M-O bond lengths near the surface are also displayed.

or Pt- electrodes on LAO/STO(001) [52] and discuss here in more detail how the electronic properties can be tuned by the metallic contact.

All the calculations presented in this Section have been performed with the full potential linearized augmented plane wave method in the *Wien2k* implementation [53] using the generalized gradient approximation GGA-PBE [54]. We have also explored the influence of an on-site Coulomb repulsion parameter (LDA/GGA+*U* method [55]) with $U = 5$ eV and $J = 1$ eV for the Ti 3d orbitals, and $U = 7$ eV for the La 4f orbitals. The irreducible part of the Brillouin zone was sampled with 21 k-points. The systems were modeled by a symmetric slab, with a 2 and 4 ML LAO film on a TiO₂-terminated STO substrate with a lateral lattice parameter set to the GGA-value of bulk STO (3.92 Å). The influence of the substrate thickness was probed by using a system with a thin (2.5 ML) and thick (6.5) ML STO slab. The metal atoms were adsorbed on top of the oxygen atoms in the top AlO₂ layer. These sites were found to be energetically favorable in previous studies of metallic overlayers on LAO(001) [56] and for other transition metal / perovskite oxide interfaces [57, 58, 59]. Further metallic layers are deposited assuming a fcc stacking of the layers. A vacuum of at least 10 Å was used to separate the supercell from its periodic images and avoid spurious interactions. The atomic positions were relaxed within tetragonal symmetry. A side view of the relaxed systems with an Al (1 ML), Ti (1 and 2 ML) and Pt (1 ML) overlayer is shown in Fig. 9.

5.1. Impact of the contact layer on the electronic properties. As discussed in Section 2, in the *n*LAO/STO(001) system a central feature is the upward shift of the O2p bands within the polar LAO film. The layer resolved DOS of Al, Ti and Pt contact layers on top of 2ML LAO/STO(001) are shown in Fig. 10. Upon adsorption of the metal overlayer this potential build up is largely canceled. Only in the case of Pt there is some residual shift of the unoccupied La 4d and 5f bands. In all cases, both the surface contact layer and the

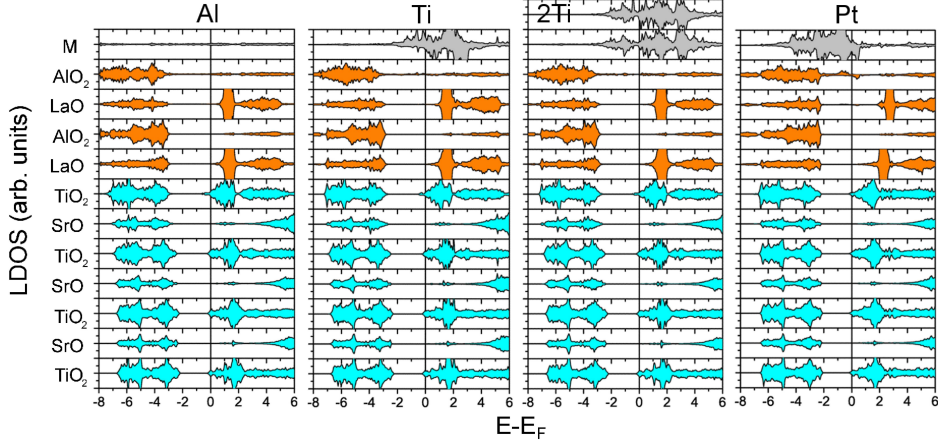


FIGURE 10. Layer resolved density of states for LAO/STO with a single ML of Al, Ti and Pt, and also with 2 ML of Ti.

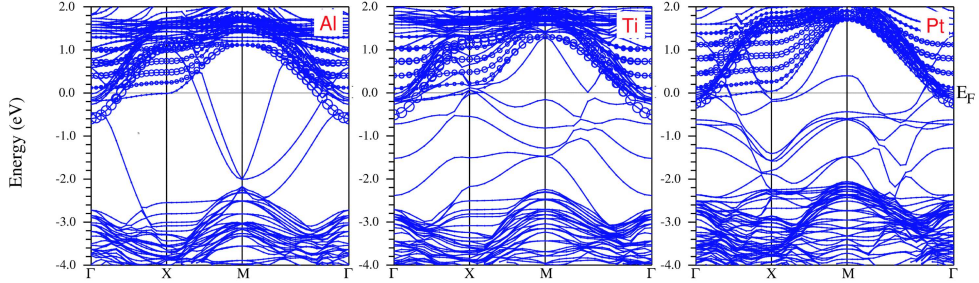


FIGURE 11. Majority spin band structures for M/LAO/STO systems (M = Al, Ti and Pt). The contribution of Ti_{3d} states at the IF layer is marked by circles.

interface layer are metallic with a significant occupation of the Ti_{3d} band at the interface and a decreasing occupation in deeper layers.

As can be seen from the band structure in Fig. 11, multiple bands contribute to conductivity: the lowest lying bands at the interface are of Ti_{3d_{xy}} character, in the IF-1 layer all t_{2g} states contribute, while in deeper layers d_{xz} , d_{yz} bands lie lowest in energy. The d_{xy} bands have a strong dispersion along $M - \Gamma - X$, whereas d_{xz} and d_{yz} are heavier along $\Gamma - X$. This difference in velocities (masses) suggests different mobilities of the carriers. Further bands between E_F and $E_F - 2.0$ eV stem from the surface metallic layer. We observe that the occupation of Ti_{3d} bands at the interface depends strongly on the type of metal contact on the surface: for an Al, Ti and Pt overlayer the band edge is 0.65, 0.5 and 0.25 eV below the Fermi level at Γ .

Further insight into the influence of the contact layer on the structural and electronic properties of LAO/STO(001) can be obtained from Fig. 12. The buckling within the layers expressed as the relative shift of anion and cation z -coordinate in Fig. 12a shows a quite different pattern compared to the systems without a metallic contact. As discussed

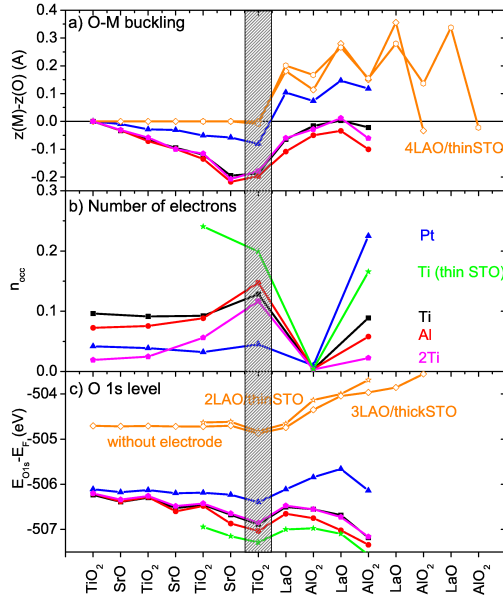


FIGURE 12. a) Oxygen-cation buckling along the [001] direction. b) Layer resolved electron occupation integrated between $E_F - 0.65$ eV and E_F . Charge on the LaO and SrO layers is zero (not shown). c) Positions of O1s states with respect to E_F . Data for 1ML Ti and thin /thick STO substrate is marked by green stars/black squares; 2ML Ti (magenta pentagons), as well as 1ML Pt (blue triangles) and 1ML Al (red circles). Results for nLAO/STO(001) without a metallic overlayer are displayed in orange with empty symbols: $n = 2, 3, 4$ ML with stars, diamonds, and hexagons, respectively.

in Section 2, in the uncovered LAO films on STO(001) the lattice polarization is confined to the LAO film where it plays a decisive role to counteract the divergence of the electric potential, while the buckling is negligible within the STO substrate (see orange lines). In contrast, after adsorbing the metallic overlayer, the potential build up in LAO is canceled and hence the anion cation buckling is strongly reduced in size (Pt contact) and even changes sign (Al and Ti overlayer).

Surprisingly at first sight, a notable polarization emerges within STO that is strongest at the interface and decays in deeper layers, similar to the one in LTO/STO and LAO/STO superlattices with an n -type interface [60, 61]. This lattice polarization in STO correlates directly with the occupation of Ti 3d bands (Fig. 12b), which is highest in the interface TiO_2 layer and decays in deeper layers. Concerning the chemical effects of the overlayer, the lattice polarization and band occupation at the interface are highest for the system with an Al overlayer, followed by Ti and lowest for a Pt overlayer, so the lattice polarization varies monotonically with the Ti 3d occupation. The position of O1s level, which is a monitor of the local potential, shows a similar trend with the strongest binding energy in the interface TiO_2 layer for an Al contact layer. The strength in binding to the surface is reflected also in the M-O bond lengths, Al-O being the shortest (1.97Å), followed by Ti-O (2.00Å) and Pt-O being longest (2.31Å) (see Fig. 9).

TABLE 1. Calculated M-O bond lengths, Ti-O buckling (difference in z -coordinate between cations and oxygen) and Ti 3d band occupation in the interface layer, integrated between E_F -0.65 eV and E_F . Work functions and Schottky barrier heights for the different contact overlayers are also displayed. For the n -SBH we give both the value obtained from the LDOS and also considering the experimental value of the LAO band gap (in brackets).

Metallic Layer	O-M distance (Å)	$z_{\text{Ti}} - z_{\text{O}}$ (IF) (Å)	n_{occ}	Φ (eV)	p -SBH (eV)	n -SBH (eV)
Al	1.97	-0.20	0.15	3.53	3.0	0.7 (2.6)
Ti	2.00	-0.19	0.13	4.05	2.8	0.9 (2.8)
2Ti	2.06	-0.18	0.11	4.05	2.8	0.9 (2.8)
Pt	2.31	-0.08	0.04	5.60	2.2	2.0 (3.4)

Dependence on the metallic contact thickness To investigate the dependence on the metallic contact thickness, we have varied the thickness of the Ti overlayer. The calculations for 2ML Ti/2LAO/STO(001) show a similar occupation of the Ti 3d band at the interface but a stronger band bending in the deeper layers leading to a lower total number of electrons within STO. This seems to correlate with a slightly larger distance between Ti in the contact layer and oxygen in the top AlO_2 layer of 2.00 Å vs. 2.06 Å for 1ML and 2ML Ti/2LAO/STO(001), respectively.

Schottky barriers Another illuminating characteristic of the M/LAO/STO(001) system, important for understanding the various band lineups and for device applications, are the Schottky barrier heights. As displayed in Table 1 these correlate again with the strength of the chemical bond and the work function: Al has the highest p -SBH (3.0 eV), followed by Ti (2.8 eV) and finally Pt (2.2 eV). As the well-known underestimation of band gaps within GGA is mostly related to the position of the conduction band minimum, n -SBH tend to be too small. Taking the experimental band gap of LAO, the n -SBH are 2.6 eV (Al), 2.8 eV (Ti) and 3.4 eV (Pt). The relevance of the chemical bonding between M and LAO/STO(001) is in line with previous findings for metal-oxide interfaces [62] that these can enhance the ferroelectricity instability in oxide capacitors.

Fig. 13 displays the schematic band diagrams of three distinct mechanisms of formation of a q2DEG discussed so far: LAO/STO(001), STO/LAO/STO(001) and M/LAO/STO(001). For LAO/STO(001) a thickness dependent IMT occurs as a result of the potential buildup, where the electronic reconstruction involves the formation of holes at the surface and electrons at the interface. In STO/LAO/STO(001) due to an additional surface state in the top TiO_2 layer the IMT takes place at a much lower LAO critical thickness and the reconstruction involves again holes in the surface layer and electrons at the interface. In contrast, for M/LAO/STO(001) the potential in LAO is flat regardless of the LAO or STO thickness. Simultaneously, a q2DEG with higher carrier density is formed at the interface. Only in the case of Pt (and possibly other noble metals), likely due to the weaker bonding and smaller charge transfer to the oxide layer, a small residual slope within LAO is found, consistent with the recently measured potential build up in Pt/LAO/STO(001) [46].

The evolution of the system due to deposition of the contact can be considered in several steps. Beginning with the internal field in 2ML LAO/STO(001) [\sim 0.8 eV potential rise], the metal layer is added and allowed to equilibrate with the outer LAO layer, determining the work function and the Schottky barrier (contact Fermi level with respect to the LAO band edges). Based on the final result shown in Fig. 10, the contact Fermi level

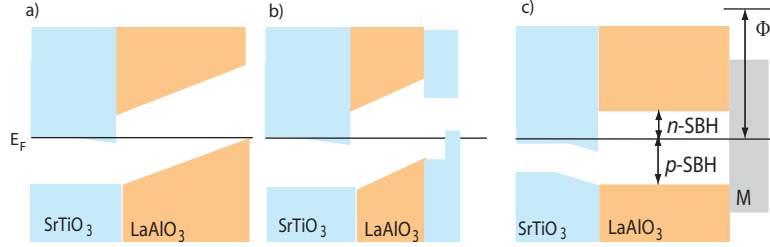


FIGURE 13. Schematic band diagram of a) LAO/STO(001) at the verge of an electronic reconstruction at the critical LAO thickness; b) LAO/STO(001) covered by an STO overlayer which leads to MIT already at 2 ML LAO and c) a metallic contact layer (M). Note, that the potential build up that leads to an electronic reconstruction in a) and b) beyond a critical LAO thickness is eliminated in M/LAO/STO(001).

would be ~ 1 eV above the STO conduction band minimum. Now, allowing exchange of charge with the interface – full self-consistency – electrons will flow from the contact layer to the interface until the Fermi levels coincide. This process is an involved one, in which the internal field and accompanying ionic polarization decrease as the charge is transferred. The determining factor is the lineup of the surface and interface Fermi levels which is accompanied by the (near-)vanishing of the electric field within the LAO slab. This charge transfer between the metal and the surface AlO₂ layer, leaving a slightly positive contact layer, will renormalize the work function of the metal and Schottky barrier somewhat. The self-consistent calculation gives only this final result, shown in Fig. 10.

5.2. Thin SrTiO₃ substrate: Spin polarization. While the results for M/LAO/STO(001) presented above were obtained using a 6.5 ML STO substrate, we have also performed calculations with a thin (2.5 ML) STO and observe there interesting confinement effects that will be described in the following. As shown in Fig. 12b a much higher Ti 3d band occupation is obtained at the interface for the thin STO substrate. However, the most prominent effect is a spin polarization of the q2DEG at the interface for the thin STO substrate. When adsorbing a single Ti layer, Ti displays a significant magnetic moment of $0.6\mu_B$ due to the reduced coordination of the metal atom at the surface. We note that also a single Pt overlayer is spin-polarized due to polarization of the holes in the 5d shell. For a Ti overlayer, this effect induces a moment of 0.10 (0.24) μ_B at the Ti sites in IF (IF-1) layer. The values obtained within GGA+*U*, where effects of strong intra-atomic interaction are included, are enhanced: 0.20 (0.30) μ_B in IF (IF-1). Such polarization seems surprising since the interface and surface layers are separated by the insulating LAO slab, precluding (or vastly reducing) exchange coupling between the layers but indeed the effect depends in the LAO spacer thickness: An increase of the width of the LAO layer reduces the influence of the contact layer expressed in a decrease of spin polarization of the q2DEG: for 1ML of Ti and 4 u.c. width of LAO calculated moments are indeed smaller ($0.05/0.11\mu_B$ for IF/IF-1).

This spin-polarization is a result of two effects. First, the fact that spin-up and spin-down Fermi levels at the surface and interface must be separately aligned (as well as with each other, finally). Second, a quantum confinement effect creates discrete bands and a

classical confinement effect leads to enhanced charge occupation at the IF and IF-1 layers. The magnetic moment of Ti in the surface contact layer is approximately $0.6\mu_B$ but decreases once the contact thickness is increased to 2 ML: the magnetic moment of the surface and subsurface Ti layer is reduced to $0.24\mu_B$ and $0.05\mu_B$ respectively due to the enhanced Ti coordination. For other electrodes with lower surface magnetic moment, like for example 1 ML of Al (no magnetic moment) or 2 ML of Ti, the spin-polarization of the q2DEG is quenched.

6. Broader Functionalities of these Interfacial Systems

The range of unexpected phenomena that has been observed in these nanostructures has systematically been broadened by new discoveries. In the preceding sections we have discussed how unusual properties, such as two-type carrier conduction or magnetism, may arise in these nanostructures. These theoretical studies are based, with a few exceptions, on atomically abrupt, structurally ideal, choices of the heterostructuring. It is understood that most if not all samples are more complicated than this. We provide here an overview of the discoveries of magnetism at the interface, then the reports of superconductivity, and finally of recent reports of coexistence of these two distinct, and usually strongly competing, types of long-range order. Understanding these phenomena will shed light on the underlying electronic structure at and near the interface. Specifically, several of these studies point out the importance of inhomogeneities in the samples, complications that should be kept in mind and will finally have to be taken into account. From the theorist's viewpoint, this emphasizes the importance of controlling defect concentration and distribution, to allow a closer connection of theory to experiment.

6.1. Hysteresis reflecting magnetic order. Soon after the initial reports on conductivity in the LAO/STO system have raised interest and research activity on this system, Brinkman and collaborators reported magnetic hysteresis in transport properties at the LAO/STO IF of PLD-deposited films. [3] This hysteresis, and an associated large negative magnetoresistance, reflects magnetic order arising at a few Kelvins and moves this oxide interface toward spintronics applications. Even prior to this study the prospect of magnetism at this interface had been raised by Pentcheva and Pickett [63] in theoretical studies of LAO/STO superlattices with either *n* or *p*-type interfaces. The question they faced at the time was this: at the polar LAO/STO interface, there is 0.5 carrier per interface cell too many (*n*-type) or too few (*p*-type) to fill bands. Therefore the interface will be conducting unless other considerations come into play. For a *n*-type interface it was demonstrated that correlation effects within GGA+*U* give rise to a charge and orbitally ordered state with magnetic moments of $0.7\mu_B$ at the Ti^{3+} -sites. Later Zhong and Kelly [64] investigated the effects of structural distortion beyond tetragonal symmetry and its impact on charge and spin ordering, finding an antiferromagnetic ground state. The relationship of the observed magnetism (due to Ti^{3+} local moments at the *n*-type interface) to the conduction by carriers remains to be clarified. We note that samples grown at high oxygen pressure, where the effect of oxygen vacancies is minimized, are nearly insulating with a sheet resistance that is seven orders of magnitude higher [3] than the initial samples studied by Ohtomo and Hwang [1].[17] On the other hand, the *p*-type interface had been found *always* to be non-conducting, independent of growth parameters. For a defect-free interface suggested by the initial reports, Pentcheva and Pickett proposed that correlation effects on the $\text{O}2p$ orbitals, resulting in charge order of oxygen holes with a magnetic moment, provided a plausible mechanism for insulating behavior. While this is an interesting case of

d^0 -magnetism, the insulating behavior of the *p*-type interface has been generally ascribed to O vacancies [35].

The possibility of magnetism at these interfaces was highlighted in Physics Today in 2007 [65] and remains an enigma. Magnetism was further discussed by Huijben *et al.*, [17] who provided a broader overview of work on oxide IFs up to that time. Subsequently, Seri and Klein [66] reported antisymmetric magnetoresistance at this interface, and noted magnetic field induced inhomogeneous magnetism, but did not characterize it as spontaneous ferromagnetism. Ariando and collaborators [67] detected dia-, ferro- and paramagnetic signals interpreted in terms of phase separation. In particular, the ferromagnetic phase persisted beyond room temperature. Li *et al.* [6] reported magnetic effects persisting up to 200 K which raises new questions, beginning with how such apparently weak magnetism can maintain spin order to such high temperature.

6.2. Superconductivity. The observation of superconductivity at the *n*-type interface by Reyren *et al.* [2] further enriched the variety of phenomena that have been reported. The superconducting state in PLD-grown samples at intermediate pressures (10^{-4} mbar) arose below 200 mK. Since bulk *n*-type STO superconducts in that range (up to 400 mK) one might initially question how new the phenomenon really is. The magnetic field directional dependence established that the superconductivity was highly two-dimensional, so in that manner its behavior is quite unlike that of bulk STO; as a 2D system it is characterized by a 2D carrier concentration rather than a 3D one. As with the magnetism, the degree of localization around the interface, and origin and character of the carriers, have become objects of scrutiny.

Subsequent reports by Caviglia *et al.* [68] and Ben Shalom *et al.* [69] confirmed superconductivity arising at this interfacial system. The latter report where 15 unit cells of LAO were deposited with pulsed laser and the carrier density was varied with gating, mapped out a portion of the phase diagram where T_c decreases as the carrier density is increasing. Kim and collaborators [70] have studied by Shubnikov-de Haas oscillations the (presumably) related superconducting state in δ -doped STO films deposited by PLD. The doping by Nb (for Ti) was performed in a varying number of TiO_2 layers, and a 2D to 3D crossover in the superconducting state was monitored. This still very new topic of oxide interface superconductivity has been reviewed by Gariglio and Triscone. [71]

6.3. Coexistence. Historically magnetism and superconductivity were mutual anathema, but the high temperature superconductivity discovered in cuprates changed that. The latest big discovery in superconductivity, the Fe-based pnictides and chalcogenides, also display magnetic phases next to superconducting ones. These as well as some other materials classes such as heavy fermion metals, [72] raise questions about possible connections between these ordered phases. In these examples the magnetism is antiferromagnetism (or correlations). Superconductivity coexisting with *ferromagnetism* is very rare, having been reported only in the past decade or so in $RuSr_2GdCu_2O_8$ [73] and in the three uranium compounds UGe_2 , $URhGe$, and $UCoGe$. Aoki *et al.* have provided a recent overview summarizing several of the phenomena and some of the issues to account for observations. [74] There are several challenges to be overcome for superconductivity to arise in a ferromagnet (see discussion in Ref. [75]): exchange splitting of up and down bands that disrupts pairing, magnetic field disruption of superconducting order, etc. We return briefly below to some of these issues.

The first observation of coexistence, by Dikin *et al.*, [5] involved superconducting onsets around $T_c \approx 150$ mK on pulsed laser deposited (PLD) films of ten unit cells of LAO

deposited on TiO_2 -terminated STO(001) substrates. They observed hysteresis in $T_c(H)$ curves (H is the magnetic field) attributed to underlying ferromagnetic order. Their interpretation focuses on two parallel conduction channels: One consists of localized, magnetic states that are intrinsic to the interface (viz. Ti^{3+} moments, likely in the immediate interface region), while the other carriers are itinerant electrons contributed by defects (a likely candidate being oxygen vacancies). While previous reports indicated quenching of magnetism at a few Kelvin, Li *et al.* [6] report high resolution magnetic torque magnetometry measurements, showing evidence of magnetic (“superparamagnetic-like”) order up to 200 K. The superconducting signal in their samples arises below 120 mK.

Most recently (as of this writing) Bert *et al.* [4] provided a real space picture of their PLD grown films. They performed imaging with a scanning SQUID (superconducting quantum interference device) over $\sim 200 \mu\text{m}$ square regions on samples of 10 ML LAO on STO(001) substrates. They report strong inhomogeneity, with sub-micron regions of ferromagnetism in a background of paramagnetic carriers that show a diamagnetic superconducting signal around 100 mK: Thus superconductivity and magnetism coexist in the sample but not in the same region. For comparison, no magnetic dipoles were observed in a reference sample of δ -doped STO. From their transport and thermodynamic measurements, they infer that most of the intrinsic carriers ($4 \times 10^{14} \text{ cm}^{-2}$ per interface cell for an atomically perfect interface) are localized, since an order-of-magnitude fewer carriers contribute to the Hall conductivity.

Some early attempts to account for this coexistence are appearing. [76, 77, 44]. The coexistence seems an even more delicate question here than in the ferromagnetic superconductors mentioned above. The ~ 200 mK critical temperature reflects a BCS gap of a few μeV , a truly tiny energy scale which appreciable exchange splitting of the bands would overwhelm. The critical magnetic field should be very small. There are aspects of the interfaces that suggest means to avoid these pair-breakers. The magnetic electrons and the superconducting carriers may reside in different bands, requiring a generalization of models applied to the previously known ferromagnetic superconductors. Inhomogeneity or phase separation may play a role, and coexistence in the same sample may not imply local coexistence (in the same region of the sample). The superconducting state may be inhomogeneous, of the FFLO type.[78, 79]

7. Summary

The $\text{LaAlO}_3/\text{SrTiO}_3$ system shows a remarkable spectrum of electronic phenomena, some of which seem to be understood and others that require further study. We have provided an overview based on DFT results addressing how the electrostatic boundary conditions determine charge (re-)distribution and the electronic state. A variety of parameters are identified, such as the surface and interface termination and stoichiometry, the presence of metallic or oxide overlayers, as well as defects and adsorbates, that enable one to tune the electronic behavior of this system. Understanding and controlling these parameters, and especially defects, dopants [80] and adsorbates, remains a challenge that needs further attention in future theoretical and experimental studies.

We acknowledge financial support through the DFG SFB/TR80 (project C3) and grant *h0721* for computational time at the Leibniz Rechenzentrum. V. G. R. L. acknowledges financial support from CONACYT (Mexico) and DAAD (Germany). W. E. P. was supported by U.S. Department of Energy Grant No. DE-FG02-04ER46111.

Bibliography

- [1] Ohtomo, A. and Hwang, H.Y. 2004 A high-mobility electron gas at the LaAlO₃/SrTiO₃ heterointerface. *Nature*, **427**, 423. doi:10.1038/nature02308.
- [2] Reyren, N., Thiel, S., Caviglia, A.D., Kourkoutis, L.F., Hammerl, G., Richter, C., Schneider, C.W., Kopp, T., Retschi, A.S., Jaccard, D., et al. 2007 Superconducting interfaces between insulating oxides. *Science*, **317**(5842), 1196–1199. doi:10.1126/science.1146006.
- [3] Brinkman, A., Huijben, M., van Zalk, M., Huijben, J., Zeitler, U., Maan, J.C., van der Wiel, W.G., Rijnders, G., Blank, D.H.A., and Hilgenkamp, H. 2007 Magnetic effects at the interface between non-magnetic oxides. *Nature Mater.*, **6**(7), 493–496. doi:10.1038/nmat1931.
- [4] Bert, J.A., Kalisky, B., Bell, C., Kim, M., Hikita, Y., Hwang, H.Y., and Moler, K.A. 2011 Direct imaging of the coexistence of ferromagnetism and superconductivity at the LaAlO₃/SrTiO₃ interface. *Nature Physics*, **advanced online publication**. doi:10.1038/nphys2079.
- [5] Dikin, D.A., Mehta, M., Bark, C.W., Folkman, C.M., Eom, C.B., and Chandrasekhar, V. 2011 Coexistence of superconductivity and ferromagnetism in two dimensions. *Phys. Rev. Lett.*, **107**(5), 056802. doi:10.1103/PhysRevLett.107.056802.
- [6] Li, L., Richter, C., Mannhart, J., and Ashoori, R.C. 2011 Coexistence of magnetic order and two-dimensional superconductivity at LaAlO₃/SrTiO₃ interfaces. *Nature physics*, **advanced online publication**. doi:doi:10.1038/nphys2080.
- [7] Thiel, S., Hammerl, G., Schmehl, A., Schneider, C.W., and Mannhart, J. 2006 Tunable quasi-two-dimensional electron gases in oxide heterostructures. *Science*, **313**(5795), 1942–1945. doi:10.1126/science.1131091.
- [8] Cen, C., Thiel, S., Hammerl, G., Schneider, C.W., Andersen, K.E., Hellberg, C.S., Mannhart, J., and Levy, J. 2008 Nanoscale control of an interfacial metalinsulator transition at room temperature. *Nature Mater.*, **7**(4), 298–302. doi:10.1038/nmat2136.
- [9] Bi, F., Bogorin, D.F., Cen, C., Bark, C.W., Park, J.W., Eom, C.B., and Levy, J. 2010 “Water-cycle” mechanism for writing and erasing nanostructures at the LaAlO₃/SrTiO₃ interface. *Appl. Phys. Lett.*, **97**, 173110. doi:10.1063/1.3506509.
- [10] Chen, Y.Z., Zhao, J.L., Sun, J.R., Pryds, N., and Shen, B.G. 2010 Resistance switching at the interface of LaAlO₃/SrTiO₃. *Appl. Phys. Lett.*, **97**, 123102. doi:10.1063/1.3490646.
- [11] Cen, C., Thiel, S., Mannhart, J., and Levy, J. 2009 Oxide nanoelectronics on demand. *Science*, **323**(5917), 1026–1030. doi:10.1126/science.1168294.
- [12] Bogorin, D.F., Irvin, P., Cen, C., and Levy, J. 2010 LaAlO₃/SrTiO₃-Based device concepts. *arXiv:1011.5290v1*.
- [13] Pentcheva, R., Huijben, M., Otte, K., Pickett, W.E., Kleibeuker, J.E., Huijben, J., Boschker, H., Kockmann, D., Siemons, W., Koster, G., et al. 2010 Parallel electron-hole bilayer conductivity from electronic interface reconstruction. *Phys. Rev. Lett.*, **104**(16), 166804. doi:10.1103/PhysRevLett.104.166804.
- [14] Hwang, H.Y. 2006 Tuning interface states. *Science*, **313**(5795), 1895–1896. doi:10.1126/science.1133138.
- [15] J. Goniakowski, F.F. and Noguera, C. 2008 Polarity of oxide surfaces and nanostructures. *Rep. Prog. Phys.*, **71**(1), 016501. doi:10.1088/0034-4885/71/1/016501.
- [16] Pauli, S.A. and Willmott, P.R. 2008 Conducting interfaces between polar and non-polar insulating perovskites. *J. Phys.: Condens. Matter*, **20**(26), 264012. doi:10.1088/0953-8984/20/26/264012.
- [17] Huijben, M., Brinkman, A., Koster, G., Rijnders, G., Hilgenkamp, H., and Blank, D.H.A. 2009 Structureproperty relation of SrTiO₃/LaAlO₃ interfaces. *Adv. Mater.*, **21**(17), 1665–1677. doi:10.1002/adma.200801448.
- [18] Pentcheva, R. and Pickett, W.E. 2010 Electronic phenomena at complex oxide interfaces: insights from first principles. *J. Phys.: Condens. Matter*, **22**, 043001. doi:10.1088/0953-8984/22/4/043001.
- [19] Chen, H., Kolpak, A.M., and Ismail-Beigi, S. 2010 Electronic and magnetic properties of SrTiO₃/LaAlO₃ interfaces from first principles. *Adv. Mater.*, **22**(26-27), 2881–2899. doi:10.1002/adma.200903800.

- [20] Zubko, P., Gariglio, S., Gabay, M., Ghosez, P., and Triscone, J.M. 2011 Interface physics in complex oxide heterostructures. *Annu. Rev. Condens. Matter Phys.*, **2**, 141–165. doi:10.1146/annurev-conmatphys-062910-140445.
- [21] Stengel, M. 2011 First-principles modeling of electrostatically doped perovskite systems. *Phys. Rev. Lett.*, **106**, 136803.
- [22] Xie, Y., Bell, C., Yajima, T., Hikita, Y., and Hwang, H.Y. 2010 Charge writing at the LaAlO₃/SrTiO₃ surface. *Nano Lett.*, **10**(7), 2588–2591. doi:10.1021/nl1012695.
- [23] Segal, Y., Ngai, J.H., Reiner, J.W., Walker, F.J., and Ahn, C.H. 2009 X-ray photoemission studies of the metal-insulator transition in LaAlO₃/SrTiO₃ structures grown by molecular beam epitaxy. *Phys. Rev. B*, **80**(24), 241107. doi:10.1103/PhysRevB.80.241107.
- [24] Sing, M., Berner, G., Goß, K., Müller, A., Ruff, A., Wetscherek, A., Thiel, S., Mannhart, J., Pauli, S.A., Schneider, C.W., et al. 2009 Profiling the interface electron gas of LaAlO₃/SrTiO₃ heterostructures with hard X-ray photoelectron spectroscopy. *Phys. Rev. Lett.*, **102**(17), 176805. doi:10.1103/PhysRevLett.102.176805.
- [25] Chambers, S., Engelhard, M., Shutthanandan, V., Zhu, Z., Droubay, T., Qiao, L., Sushko, P., Feng, T., Lee, H., Gustafsson, T., et al. 2010 Instability, intermixing and electronic structure at the epitaxial heterojunction. *Surface Science Reports*, **65**(10–12), 317 – 352. ISSN 0167-5729. doi:DOI: 10.1016/j.surrep.2010.09.001.
- [26] Zhong, Z., Xu, P.X., and Kelly, P.J. 2010 Polarity-induced oxygen vacancies at LaAlO₃/SrTiO₃ interfaces. *Phys. Rev. B*, **82**(16), 165127. doi:10.1103/PhysRevB.82.165127.
- [27] Bristowe, N.C., Littlewood, P.B., and Artacho, E. 2011 Surface defects and conduction in polar oxide heterostructures. *Phys. Rev. B*, **83**(20), 205405. doi:10.1103/PhysRevB.83.205405.
- [28] Son, W., Cho, E., Lee, J., and Han, S. 2010 Hydrogen adsorption and carrier generation in LaAlO₃-SrTiO₃ heterointerfaces: A first-principles study. *J. Phys.: Condens. Matter*, **22**(31), 315501. doi:10.1088/0953-8984/22/31/315501.
- [29] Willmott, P.R., Pauli, S.A., Herger, R., Schlepütz, C.M., Martoccia, D., Patterson, B.D., Delley, B., Clarke, R., Kumah, D., Cionca, C., et al. 2007 Structural basis for the conducting interface between LaAlO₃ and SrTiO₃. *Phys. Rev. Lett.*, **99**(15), 155502. doi:10.1103/PhysRevLett.99.155502.
- [30] Qiao, L., Droubay, T.C., Shutthanandan, V., Zhu, Z., Sushko, P.V., and Chambers, S.A. 2010 Thermodynamic instability at the stoichiometric LaAlO₃/SrTiO₃(001) interface. *J. Phys.: Condens. Matter*, **22**, 312201. doi:10.1088/0953-8984/22/31/312201.
- [31] Ishibashi, S. and Terakura, K. 2008 Analysis of screening mechanisms for polar discontinuity for LaAlO₃/SrTiO₃ thin films based on *Ab initio* calculations. *J. Phys. Soc. Jpn.*, **77**(10), 104706.
- [32] Pentcheva, R. and Pickett, W.E. 2009 Avoiding the polarization catastrophe in LaAlO₃ over-layers on SrTiO₃(001) through polar distortion. *Phys. Rev. Lett.*, **102**(10), 107602. doi:10.1103/PhysRevLett.102.107602.
- [33] Son, W.j., Cho, E., Lee, B., Lee, J., and Han, S. 2009 Density and spatial distribution of charge carriers in the intrinsic *n*-type LaAlO₃–SrTiO₃ interface. *Phys. Rev. B*, **79**(24), 245411. doi:10.1103/PhysRevB.79.245411.
- [34] Pauli, S.A., Leake, S.J., Delley, B., Björck, M., Schneider, C.W., Schlepütz, C.M., Martoccia, D., Paetel, S., Mannhart, J., and Willmott, P.R. 2011 Evolution of the interfacial structure of LaAlO₃ on SrTiO₃. *Phys. Rev. Lett.*, **106**(3), 036101. doi:10.1103/PhysRevLett.106.036101.
- [35] Nakagawa, N., Hwang, H.Y., and Muller, D.A. 2006 Why some interfaces cannot be sharp. *Nature Mater.*, **5**, 204–209. doi:10.1038/nmat1569.
- [36] Pavlenko, N. and Kopp, T. 2004 Structural relaxation and metal-insulator transition at the interface between SrTiO₃ and LaAlO₃. *Surface Science*, **605**, 1114–1121. doi:10.1016/j.susc.2011.03.016.
- [37] Huijben, M., Rijnders, G., Blank, D.H.A., Bals, S., Van Aert, S., Verbeeck, J., Van Tendeloo, G., Brinkman, A., and Hilgenkamp, H. 2006 Electronically coupled complementary interfaces between perovskite band insulators. *Nature Mater.*, **5**(7), 556–560. doi:10.1038/nmat1675.
- [38] Padilla, J. and Vanderbilt, D. 1998 Ab initio study of SrTiO₃ surfaces. *Surface Science*, **418**(1), 64–70. doi:10.1016/S0039-6028(98)00670-0.
- [39] Kimura, S., Yamauchi, J., Tsukada, M., and Watanabe, S. 1995 First-principles study on electronic structure of the (001) surface of SrTiO₃. *Phys. Rev. B*, **51**(16), 11049–11054. doi:10.1103/PhysRevB.51.11049.
- [40] Takizawa, M., Tsuda, S., Susaki, T., Hwang, H.Y., and Fujimori, A. 2011 Electronic charges and electric potential at LaAlO₃/SrTiO₃ interfaces studied by core-level photoemission spectroscopy. *arXiv:1106.3619v1*.
- [41] Chen, H., Kolpak, A.M., and Ismail-Beigi, S. 2009 Fundamental asymmetry in interfacial electronic reconstruction between insulating oxides: An *ab initio* study. *Phys. Rev. B*, **79**, 161402. doi:10.1103/PhysRevB.79.161402.

- [42] Zhang, L., Zhou, X.F., Wang, H.T., Xu, J.J., Li, J., Wang, E.G., and Wei, S.H. 2010 Origin of insulating behavior of the *p*-type LaAlO₃/SrTiO₃ interface: Polarization-induced asymmetric distribution of oxygen vacancies. *Phys. Rev. B*, **82**(12), 125412. doi:10.1103/PhysRevB.82.125412.
- [43] Li, Y., Na Phattalung, S., Limpijumnong, S., and Yu, J. 2009 Oxygen-vacancy-induced charge carrier in n-type interface of LaAlO₃ overlayer on SrTiO₃ (001): interface vs bulk doping carrier. *arXiv:0912.4805v1*.
- [44] Pavlenko, N., Kopp, T., Y.Tsymbal, E., Sawatzky, G.A., and Mannhart, J. 2011 Magnetism and superconductivity at LAO/STO-interfaces both generated by the Ti 3d interface electrons? *arXiv:1105.1163v1*.
- [45] Jany, R., Breitschaft, M., Hammerl, G., Horsche, A., Richter, C., Paetel, S., Mannhart, J., Stucki, N., Reyren, R., Gariglio, S., et al. 2010 Diodes with breakdown voltages enhanced by the metal-insulator transition of LaAlO₃-SrTiO₃ interfaces. *Appl. Phys. Lett.*, **96**, 183504. doi:10.1063/1.3428433.
- [46] Singh-Bhalla, G., Bell, C., Ravichandran, J., Siemons, W., Hikita, Y., Salahuddin, S., Hebard, A.F., Hwang, H.Y., and Ramesh, R. 2011 Built-in and induced polarization across LaAlO₃/SrTiO₃ heterojunctions. *Nature Physics*, **7**, 80. doi:10.1038/NPHYS1814.
- [47] Campbell, C.T. 1997 Ultrathin metal films and particles on oxide surfaces: structural, electronic and chemisorption properties. *Surface Science Reports*, **27**(1-3), 1–111. doi:10.1016/S0167-5729(96)00011-8.
- [48] Goniakowski, J. and Noguera, C. 2004 Electronic states and schottky barrier height at metal/MgO(100) interfaces. *Interface science*, **12**(1), 93–103. doi:10.1023/B:INTS.0000012298.34540.50.
- [49] Duan, C.G., Jaswal, S.S., and Tsymbal, E.Y. 2006 Predicted magnetoelectric effect in Fe/BaTiO₃ multilayers: Ferroelectric control of magnetism. *Phys. Rev. Lett.*, **97**(4), 047201. doi:10.1103/PhysRevLett.97.047201.
- [50] Fu, Q. and Wagner, T. 2007 Interaction of nanostructured metal overlayers with oxide surfaces. *Surface Science Reports*, **62**(11), 431–498. doi:10.1016/j.surrep.2007.07.001.
- [51] Fechner, M., Maznichenko, I.V., Ostanin, S., Ernst, A., Henk, J., Bruno, P., and Mertig, I. 2008 Magnetic phase transition in two-phase multiferroics predicted from first principles. *Phys. Rev. B*, **78**(21), 212406. doi:10.1103/PhysRevB.78.212406.
- [52] López, V.R., Arras, R., Pickett, W., and Pentcheva, R. 2011 Tuning the two-dimensional electron gas at the LaAlO₃/SrTiO₃(001) interface by metallic contacts. *arXiv:1106.4205v1*.
- [53] Blaha, P., Schwarz, K., Madsen, G., Kvasnicka, D., and Luitz, J. WIEN2k, an augmented plane wave plus local orbitals program for calculating crystal properties. (Karlheinz Schwarz, Technische Universität Wien, Austria, 2001).
- [54] Perdew, J.P., Burke, K., and Ernzerhof, M. 1996 Generalized Gradient Approximation made simple. *Phys. Rev. Lett.*, **77**(18), 3865–3868. doi:10.1103/PhysRevLett.77.3865.
- [55] Anisimov, V.I., Solovyev, I.V., Korotin, M.A., Czyzyk, M.T., and Sawatzky, G.A. 1993 Density-functional theory and NiO photoemission spectra. *Phys. Rev. B*, **48**(23), 16929–16934. doi:10.1103/PhysRevB.48.16929.
- [56] Asthagiri, A. and Sholl, D.S. 2006 Pt thin films on the polar LaAlO₃(100) surface: A first-principles study. *Phys. Rev. B*, **73**(12), 125432. doi:10.1103/PhysRevB.73.125432.
- [57] Asthagiri, A. and Scholl, D.S. 2002 First principles study of Pt adhesion and growth on SrO- and TiO₂-terminated SrTiO₃(100). *J. Chem. Phys.*, **116**, 9914–9925. doi:10.1063/1.1476322.
- [58] Ochs, T., Köstlmeier, S., and Elsässer, C. 2001 Microscopic structure and bonding at the Pd/SrTiO₃ (001) interface an ab-initio local-density-functional study. *Integrated Ferroelectrics*, **32**(1-4), 267–278. doi:10.1080/10584580108215697.
- [59] Oleinik, I.I., Tsymbal, E.Y., and Pettifor, D.G. 2001 Atomic and electronic structure of Co/SrTiO₃/Co magnetic tunnel junctions. *Phys. Rev. B*, **65**(2), 020401. doi:10.1103/PhysRevB.65.020401.
- [60] Okamoto, S., Millis, A.J., and Spaldin, N.A. 2006 Lattice relaxation in oxide heterostructures: LaTiO₃/SrTiO₃ superlattices. *Phys. Rev. Lett.*, **97**, 056802. doi:10.1103/PhysRevLett.97.056802.
- [61] Pentcheva, R. and Pickett, W.E. 2008 Ionic relaxation contribution to the electronic reconstruction at the n-type LaAlO₃/SrTiO₃ interface. *Phys. Rev. B*, **78**, 205106. doi:10.1103/PhysRevB.78.205106.
- [62] Stengel, M., Vanderbilt, D., and Spaldin, N.A. 2009 Enhancement of ferroelectricity at metal-oxide interfaces. *Nature Mater.*, **8**, 392–397. doi:10.1038/NMAT2429.
- [63] Pentcheva, R. and Pickett, W.E. 2006 Charge localization or itineracy at LaAlO₃/SrTiO₃ interfaces: Hole polarons, oxygen vacancies, and mobile electrons. *Phys. Rev. B*, **74**(3), 035112. doi:10.1103/PhysRevB.74.035112.
- [64] Zhong, Z. and Kelly, P. 2008 Electronic-structure-induced reconstruction and magnetic ordering at the LaAlO₃/SrTiO₃ interface. *Europhys. Lett.*, **84**, 27001. doi:10.1209/0295-5075/84/27001.
- [65] Goss Levi, B. 2007 Interface between nonmagnetic insulators may be ferromagnetic and conducting. *Physics Today*, **60**, 23. doi:10.1063/1.2754590.

- [66] Seri, S. and Klein, L. 2009 Antisymmetric magnetoresistance of the SrTiO₃/LaAlO₃ interface. *Phys. Rev. B*, **80**(18), 180410. doi:10.1103/PhysRevB.80.180410.
- [67] Ariando, Wang, X., Baskaran, G., Liu, Z.Q., Huijben, J., Yi, J.B., Annadi, A., Barman, A.R., Rusydi, A., Dhar, S., et al. 2011 Electronic phase separation at the LaAlO₃/SrTiO₃ interface. *Nature Commun.*, **2**, 188. doi:10.1038/ncomms1192.
- [68] Caviglia, A.D., Gariglio, S., Reyren, N., Jaccard, D., Schneider, T., Gabay, M., Thiel, S., Hammerl, G., Mannhart, J., and Triscone, J.M. 2008 Electric field control of the LaAlO₃/SrTiO₃ interface ground state. *Nature*, **456**, 624–627. doi:10.1038/nature07576.
- [69] Ben Shalom, M., Sachs, M., Rakhmievitch, D., Palevski, A., and Dagan, Y. 2010 Tuning spin-orbit coupling and superconductivity at the SrTiO₃/LaAlO₃ interface: A magnetotransport study. *Phys. Rev. Lett.*, **104**(12), 126802. doi:10.1103/PhysRevLett.104.126802.
- [70] Kim, M., Bell, C., Kozuka, Y., Kurita, M., Hikita, Y., and Hwang, H.Y. 2011 Fermi surface and superconductivity in low-density high-mobility δ -doped SrTiO₃. *arXiv:1104.3388v2*.
- [71] Gariglio, S. and Triscone, J.M. 2011 Oxide interface superconductivity – Supraconductivité à l’interface d’oxydes. *Compt. Rend. Physiq.*, **12**(5–6), 591–599. doi:10.1016/j.crhy.2011.03.006.
- [72] Sarrao, J.L., Morales, L.A., Thompson, J.D., Scott, B.L., Stewart, G.R., Wastin, F., Rebizant, J., Boulet, P., Colineau, E., and Lander, G.H. 2002 Plutonium-based superconductivity with a transition temperature above 18 K. *Nature*, **420**, 297–299. doi:10.1038/nature01212.
- [73] Bernhard, C., Tallon, J.L., Niedermayer, C., Blasius, T., Golnik, A., Brücher, E., Kremer, R.K., Noakes, D.R., Stronach, C.E., and Ansaldi, E.J. 1999 Coexistence of ferromagnetism and superconductivity in the hybrid ruthenate-cuprate compound RuSr₂GdCu₂O₈ studied by muon spin rotation and dc magnetization. *Phys. Rev. B*, **59**(21), 14099–14107. doi:10.1103/PhysRevB.59.14099.
- [74] Aoki, D., Hardy, F., Miyake, A., Taufour, V., Matsuda, T.D., and Flouquet, J. 2011 Properties of ferromagnetic superconductors – Des supraconducteurs ferromagnétiques. *Compt. Rend. Physiq.*, **12**(5–6), 573–583. doi:10.1016/j.crhy.2011.04.007.
- [75] Pickett, W.E., Weht, R., and Shick, A.B. 1999 Superconductivity in ferromagnetic RuSr₂GdCu₂O₈. *Phys. Rev. Lett.*, **83**(18), 3713–3716. doi:10.1103/PhysRevLett.83.3713.
- [76] Michaeli, K., Potter, A.C., and A Lee, P. 2011 Superconductivity and ferromagnetism in oxide interface structures: Possibility of finite momentum pairing. *arXiv:1107.4352v2*.
- [77] Stephanos, C., Kopp, T., Mannhart, J., and Hirschfeld, P.J. 2011 Interface-induced d-wave pairing. *arXiv:1108.1942v1*.
- [78] Fulde, P. and Ferrell, R.A. 1964 Superconductivity in a strong spin-exchange field. *Phys. Rev.*, **135**(3A), A550–A563. doi:10.1103/PhysRev.135.A550.
- [79] Larkin, A.I. and Ovchinnikov, Y.N. 1964 *Zh. Eksp. Teor. Fiz.*, **47**, 1136–1146.
- [80] Fix, T., Schoofs, F., MacManus-Driscoll, J.L., and Blamire, M.G. 2009 Charge confinement and doping at LaAlO₃/SrTiO₃ interfaces. *Phys. Rev. Lett.*, **103**, 166802.